Differential Regulation of Endothelial Cell Permeability by High and Low Doses of Oxidized 1-Palmitoyl-2-Arachidonyl-*sn*-Glycero-3-Phosphocholine

Vitaliy Starosta[1], Tinghuai Wu[1], Alejandro Zimman[2], Donald Pham[2], Xinyong Tian[1], Olga Oskolkova[3], Valery Bochkov[3], Judith A. Berliner[2], Anna A. Birukova[1], and Konstantin G. Birukov[1]

[1]Lung Injury Center, Section of Pulmonary and Critical Medicine, Department of Medicine, University of Chicago, Chicago, Illinois; [2]Department of Pathology, University of California at Los Angeles, Los Angeles, California; and [3]Department of Vascular Biology and Thrombosis Research, Medical University of Vienna, Vienna, Austria

The generation of phospholipid oxidation products in atherosclerosis, sepsis, and lung pathologies affects endothelial barrier function, which exerts significant consequences on disease outcomes in general. Our group previously showed that oxidized 1-palmitoyl-2-arachidonyl-*sn*-glycero-3-phosphocholine (OxPAPC) at low concentrations increases endothelial cell (EC) barrier function, but decreases it at higher concentrations. In this study, we determined the mechanisms responsible for the pulmonary endothelial cell barrier dysfunction induced by high OxPAPC concentrations. OxPAPC at a range of 5–20 μg/ml enhanced EC barriers, as indicated by increased transendothelial electrical resistance. In contrast, higher OxPAPC concentrations (50–100 μg/ml) rapidly increased EC permeability, which was accompanied by increased total cell protein tyrosine (Tyr) phosphorylation, phosphorylation at Tyr-418, the activation of Src kinase, and the phosphorylation of adherens junction (AJ) protein vascular endothelial cadherin (VE-cadherin) at Tyr-731 and Tyr-658, which was not observed in ECs stimulated with low OxPAPC doses. The early tyrosine phosphorylation of VE-cadherin was linked to the dissociation of VE-cadherin–p120-catenin/β-catenin complexes and VE-cadherin internalization, whereas low OxPAPC doses promoted the formation of VE-cadherin–p120-catenin/β-catenin complexes. High but not low doses of OxPAPC increased the production of reactive oxygen species (ROS) and protein oxidation. The inhibition of Src by PP2 and ROS production by *N*-acetyl cysteine inhibited the disassembly of VE-cadherin–p120-catenin complexes, and attenuated high OxPAPC-induced EC barrier disruption. These results show the differential effects of OxPAPC doses on VE-cadherin–p120-catenin complex assembly and EC barrier function. These data suggest that the rapid tyrosine phosphorylation of VE-cadherin and other potential targets mediated by Src and ROS-dependent mechanisms plays a key role in the dissociation of AJ complexes and EC barrier dysfunction induced by high OxPAPC doses.

Keywords: endothelium; oxidized phospholipids; protein tyrosine phosphorylation; VE-cadherin; permeability

CLINICAL RELEVANCE

In contrast to low concentrations of oxidized phospholipids, high doses of oxidized phospholipids cause a rapid increase in endothelial permeability. This mechanism does not implicate the activation of actomyosin contraction, but involves the stimulation of the production of reactive oxygen species and the activation of Src kinase, leading to the phosphorylation of vascular endothelial cadherin, the disassembly of cell–cell junction complexes, and endothelial monolayer barrier compromise. An understanding of signaling pathways triggered by circulating oxidized phospholipids is important for the development of therapeutic options in the treatment of lung diseases associated with impaired redox balance and inflammation.

Oxidative stress and the activation of phospholipases lead to the formation and accumulation of biologically active lipid oxidation products. Phospholipid oxidation products were shown to accumulate in a number of inflammatory diseases (1). An increase in oxidative stress and in phospholipid oxidation products was demonstrated in patients with diverse lung diseases, such as acute respiratory distress syndrome, ventilator-induced lung injury, and asthma, and in animal studies of lung injury (2–4). Oxidized phospholipids were also shown to accumulate in atherosclerosis and other chronic inflammatory diseases (5). The increased concentrations of oxidized phospholipids in the injured lung may influence the functions of pulmonary endothelial cells (ECs), including the modulation of pulmonary inflammatory response and EC barrier regulation (6–9).

Oxidized phospholipids may induce various proinflammatory effects, including the stimulation of cytokines and chemokine production (10, 11), the activation of cell adhesion molecules (12, 13), the elevation of intracellular and extracellular levels of superoxide radicals in human ECs (14, 15), the activation of coagulation cascades, and platelet activation (16, 17). However, in addition to tissue-damaging and proinflammatory effects, oxidized phospholipid products may exhibit potent anti-inflammatory activities under certain conditions. Oxidized 1-palmitoyl-2-arachidonoyl-*sn*-glycero-3-phosphatidyl choline (OxPAPC) may inhibit the tissue oxidative burst induced by bacterial compounds, induce anti-inflammatory and antioxidant genes, and protect lung tissue from LPS-induced lung injury (9, 18).

In vitro and *in vivo* studies showed contradictory effects of OxPAPC on monolayer permeability in cultured ECs and models of acute lung injury. OxPAPC exhibited potent barrier-protective effects on human pulmonary ECs, which were mediated by the small GTPases Rac and Cdc42 (19). Adherens junctions (AJs) play a major role in the regulation of endothelial permeability. AJs are largely composed of vascular endothelial (VE) cadherin, an endothelium-specific member of the cadherin family of adhesion proteins that binds, via its cytoplasmic domain, to several protein partners, including p120-catenin

(*Received in original form May 10, 2011 and in final form October 8, 2011*)

This work was supported by National Heart, Lung, and Blood Institutes grants HL87823 (K.G.B.), HL76259 (K.G.B.), PO1 HL58064 (K.G.B.), HL89257 (A.A.B.), HL107920 (A.A.B.), and PO1 HL030568 (J.A.B.).

Correspondence and requests for reprints should be addressed to Konstantin G. Birukov, M.D., Ph.D., Lung Injury Center, Section of Pulmonary and Critical Medicine, Department of Medicine, University of Chicago, 5841 S. Maryland Ave., Office N611, Chicago, IL 60637. E-mail: kbirukov@medicine.bsd.uchicago.edu

Am J Respir Cell Mol Biol Vol 46, Iss. 3, pp 331–341, Mar 2012

Originally Published in Press as DOI: 10.1165/rcmb.2011-0153OC on October 13, 2011
Internet address: www.atsjournals.org

and β-catenin (20). OxPAPC was also shown to induce the translocation and peripheral accumulation of focal adhesion complexes, and an increased association with VE-cadherin, p120-catenin, α-catenin, β-catenin, and γ-catenin leads to cell-junction enhancement and an increase in the area covered by AJs (21). Using measurements of the transendothelial electrical resistance of endothelial monolayers *in vitro*, we showed that the stimulation of pulmonary ECs with OxPAPC doses in the range of 5–20 μg/ml increased basal EC monolayer barrier properties in a dose-dependent manner. Moreover, the addition of OxPAPC to pulmonary EC culture treated with the edemagenic agonist thrombin accelerated the recovery of thrombin-induced EC barrier disruption, but at high concentrations, OxPAPC caused barrier disruption (19, 22). *In vivo* studies demonstrated that OxPAPC significantly improved lung vascular barrier properties in a murine model of ventilator-induced lung injury (8). However, in another model of lung injury involving acid treatment, OxPAPC accelerated lung injury and inflammation (6). Furthermore, inflammation was associated with increases of OxPAPC during influenza virus infection in humans (6).

The differential effects of high and low OxPAPC doses pose intriguing questions in vascular biology, with important implications in the regulation of the vascular endothelial barrier in chronic (atherosclerosis) and acute (acute lung injury and sepsis) pathologic conditions, and understanding the doses and signaling mechanisms triggering these responses is of great importance. Understanding the dose-dependent effects of oxidized phospholipids (OxPLs) on the vascular endothelial barrier is also important in light of the controversy regarding the beneficial effects of exogenous OxPL formulations administered via intravenous, intratracheal, or subcutaneous routes and at various doses, as reported by different groups, and the deleterious effects associated with elevations of endogenous OxPL concentrations.

Our previous work described signaling cascades and identified a number of cellular targets mediating the barrier-protective effects of low OxPAPC doses (23, 24). This study evaluates the pathways differentially activated by high and low OxPAPC doses, to characterize the less well-understood mechanisms of EC barrier disruption induced by increased OxPAPC concentrations. We tested the hypothesis that the early barrier-disruptive effects of high OxPAPC doses are mediated by a redox-dependent tyrosine phosphorylation of VE-cadherin, leading to the dissociation of VE-cadherin–containing cell junction complexes.

MATERIALS AND METHODS

Cell Culture and Reagents

Human pulmonary artery endothelial cells (HPAECs) were obtained from Lonza (Allendale, NJ), and used at passages 5–8. All experiments were performed in endothelial cell growth medium (EGM) (Lonza) containing 2% FBS, unless otherwise specified. Texas Red–conjugated phalloidin and Alexa Fluor 488–labeled secondary antibodies were purchased form Molecular Probes (Eugene, OR). Primary 4G10 anti-phosphotyrosine antibodies were purchased from Millipore (Billerica, MA). We purchased p120-catenin and β-catenin from BD Transduction Laboratories (San Diego, CA), phospho-Src and phospho–VE-cadherin antibodies from Invitrogen (Carlsbad, CA), and VE-cadherin from Santa Cruz Biotechnology (Santa Cruz, CA). The PP2 inhibitor (4-amino-5-(4-chlorophenyl)-7-(*t*-butyl)pyrazolo[3,4-d]pyrimidine) was purchased from Calbiochem (La Jolla, CA). Unless otherwise specified, all biochemical reagents were obtained from Sigma (St. Louis, MO). 1-Palmitoyl-2-arachidonoyl-*sn*-glycero-3-phosphatidyl choline (PAPC) was purchased from Avanti Polar Lipids (Alabaster, AL). The oxidation of PAPC was performed by exposing dry lipid to air, as previously described (25).

Immunofluorescence Microscopy

HPAECs grown to 95–100% confluence on gelatinized coverslips were stimulated with the agonist of interest, followed by immunofluorescence staining as previously described (19). The analysis of immunofluorescence staining was performed using an Olympus IX71 microscope with a ×60 objective lens (Olympus, Tokyo, Japan).

Measurement of Reactive Oxygen Species

HPAECs were grown in 96-well plates, and 5-(and -6)-carboxy-2′,7′-dichlorodihydrofluorescein diacetate was added, to achieve a final concentration of 10 μM. Cells were incubated in serum-free medium for 30 minutes at 37°C, protected from light, and then stimulated with OxPAPC. The measurement of reactive oxygen species (ROS) was performed using the Image-iT LIVE Green Reactive Oxygen Species Detection Kit from Molecular Probes, according to the manufacturer's instructions.

Measurement of Protein Oxidation

The evaluation of intracellular protein oxidation involved the detection of protein carbonylation with an OxyBlot Protein Oxidation Kit (Millipore), according to the manufacturer's protocol.

Cell viability was assessed using the LIVE/DEAD Assay (Molecular Probes) according to the manufacturer's instructions, as previously described (26).

Surface Protein Biotinylation

Cells were washed with PBS (at 37°C) and incubated with Sulfo-NHS-SS-Biotin (Pierce Biotechnology, Rockford, IL) (5 mM, 10 min at room temperature). Subsequently, cells were washed twice with 100 mM glycine/PBS, lysed in 1% Triton-100/PBS (30 minutes, on ice), and centrifuged (10,000 × *g*, 10 min, at 4°C). Equal amounts of lysates were incubated with 60 μl of streptavidin–agarose (Pierce Biotechnology) (1 hour at 4°C). Beads were washed three times with ice-cold PBS and boiled in sodium dodecyl sulfate sample buffer with 5% 2-mercaptoethanol. Samples were centrifuged for 1 minute at 1,000 × *g*, and supernatants were subjected to Western blotting with VE-cadherin antibody.

Measurement of Transendothelial Electrical Resistance

Measurements of transendothelial electrical resistance (TER) across confluent HPAEC monolayers were performed using an electrical cell-substrate impedance sensing system from Applied Biophysics (Troy, NY), as previously described (27).

Immunoprecipitation

Cells were stimulated with OxPL according to experimental conditions, followed by immunoprecipitation under nondenaturing conditions. Immunoprecipitates were subjected to Western blot analysis, as described elsewhere (27).

Statistical Analysis

The results are expressed as the means ± SD of 3–5 independent experiments. Stimulated samples were compared with control samples, using the unpaired Student *t* test. For multiple-group comparisons, one-way ANOVA and *post hoc* multiple comparisons tests were used. $P < 0.05$ was considered statistically significant.

RESULTS

Differential Effects of High and Low OxPAPC Doses on Endothelial Barrier Function

The dose-dependent effects of OxPAPC on EC permeability were assessed by measurements of TER. OxPAPC at concentrations of 1–20 μg/ml gradually enhanced EC barriers (Figure 1A), and the barrier-enhancing response lasted for several hours. In contrast, higher doses of OxPAPC, ranging from

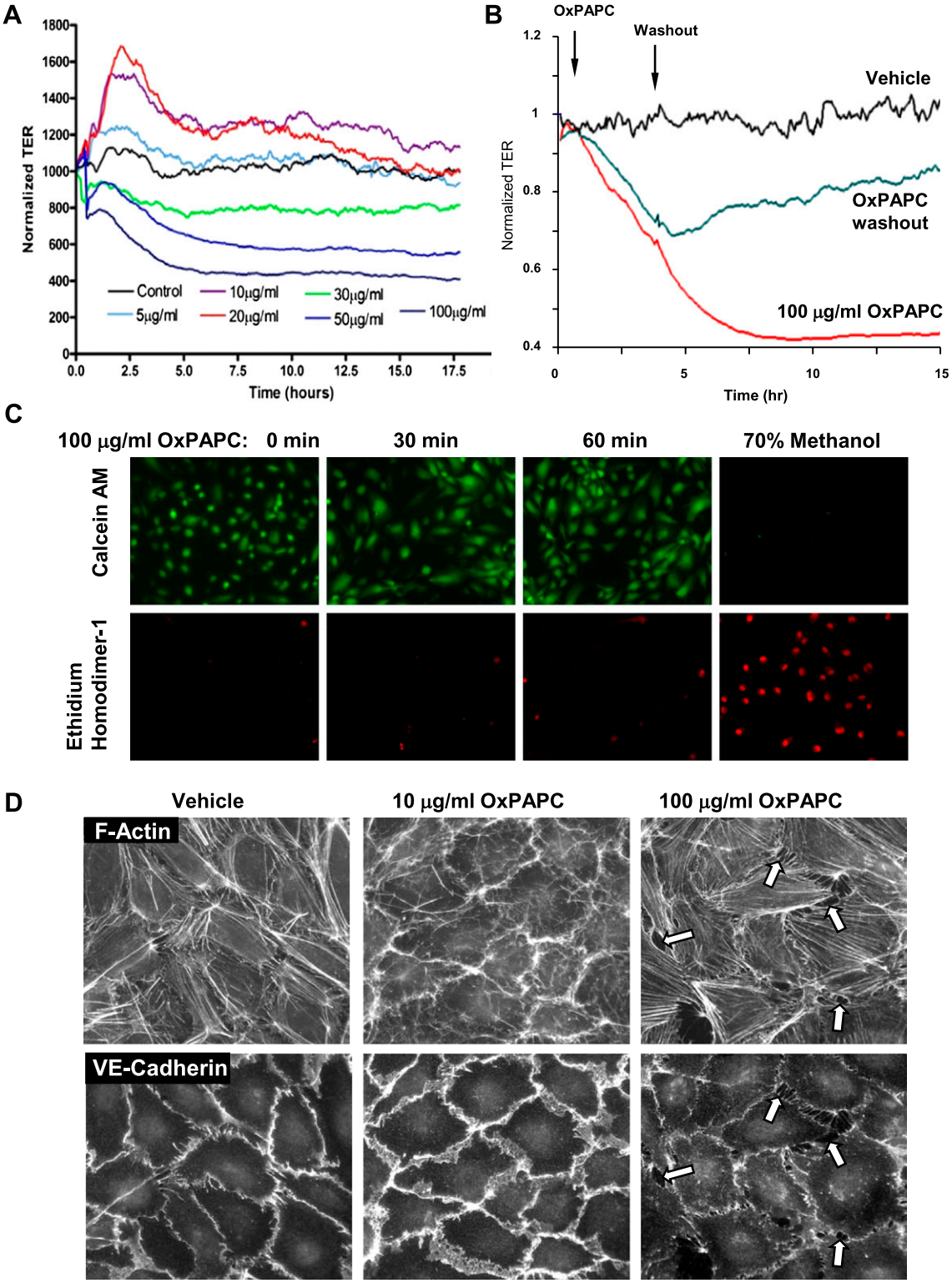

Figure 1. Dose-dependent effects of oxidized 1-palmitoyl-2-arachidonyl-*sn*-glycero-3-phosphocholine (OxPAPC) on transendothelial electrical resistance (TER) and endothelial monolayer integrity. (*A*) Human pulmonary artery endothelial cells (HPAECs) were seeded in polycarbonate wells with gold microelectrodes. After 24 hours of culture, HPAECs were stimulated with various OxPAPC concentrations (5, 10, 20, 30, 50, and 100 μg/ml) or vehicle, and measurements of TER were monitored for 18 hours, using an electrical cell-substrate impedance sensing system. The results are representative of five independent experiments. (*B*) After exposure to 100 μg/ml OxPAPC and TER measurements, the culture medium was replaced by a fresh serum-free medium without OxPAPC, and TER changes in endothelial cell (EC) monolayers grown on microelectrodes were monitored over an additional period of time. The removal of OxPAPC from the culture medium partly restored TER in HPAEC monolayers. (*C*) Effects of 100 μg/ml OxPAPC on HPAEC viability. Cells were subjected to 100 μg/ml OxPAPC for 4 hours, and cell viability was assessed as described in Materials and Methods. Methanol treatment was used as a positive control for cell death. (*D*) Endothelial monolayers grown on glass coverslips were stimulated with OxPAPC (10 μg/ml or 100 μg/ml) for 30 minutes, followed by double immunofluorescence staining for F-actin or vascular endothelial cadherin (VE-cadherin). *Arrows* indicate areas of intercellular gaps caused by treatment with 100 μg/ml OxPAPC. The results shown are representative of three independent experiments. AM, acetoxymethyl.

30–100 μg/ml, caused a dose-dependent sustained decrease in TER, reflecting increased EC permeability for up to 5 hours. Previous studies using similar OxPAPC concentrations showed a lack of OxPAPC toxicity on ECs (28). We performed additional analyses in this study, and showed that replacing the medium after OxPAPC treatment with fresh serum-free medium partly restored barrier properties of EC monolayers (Figure 1B), suggesting the reversibility of OxPAPC's barrier-disruptive effects. Furthermore, the addition of EGM containing 2% FCS increased TER above basal levels (data not shown). In additional experiments, the LIVE/DEAD Assay was performed. Ethidium homodimer–1 (red fluorescence) is excluded by the intact plasma membrane of live cells, and labels the nuclear DNA of dead cells. Calcein-acetoxymethyl (green fluorescence) is a cell-permeant dye retained within live cells. In agreement with those results, OxPAPC at 100 μg/ml was not toxic to cells, as determined by a cell viability assay (Figure 1C). The immunofluorescence staining of F-actin and the AJ protein VE-cadherin in HPAEC monolayers treated with barrier-enhancing and barrier-disruptive OxPAPC concentrations showed distinct patterns of cytoskeletal and AJ remodeling. Lower OxPAPC doses (10 μg/ml) induced a peripheral accumulation of F-actin and increased VE-cadherin–positive areas at cell–cell junctions, indicating enhanced AJs. In contrast, exposure to higher OxPAPC doses (100 μg/ml) caused the formation of intercellular gaps (Figure 1D, *arrows*), the appearance of central F-actin fibers, and a significant reduction of VE-cadherin immunoreactivity at cell–cell junctions (Figure 1D, *below*), reflecting decreased EC monolayer barrier function.

Effects of OxPAPC on ROS Generation and Protein Oxidation

Treatment with 100 μg/ml OxPAPC increased ROS production in HPAECs (Figure 2A), compared with ROS production in ECs treated with 10 μg/ml OxPAPC. Notably, the production of ROS induced by high OxPAPC doses was considerably lower, compared with the production of ROS in ECs pretreated with 100 μM H_2O_2, which was used as a positive control. The effects of OxPAPC on cellular oxidation were further evaluated by an analysis of protein oxidation, using oxyblot techniques described in MATERIALS AND METHODS. The treatment of ECs with 100 μg/ml OxPAPC increased protein carbonylation in a time-dependent manner, reflecting protein oxidation, whereas low OxPAPC concentrations were without effect (Figure 2B). The stimulation of ECs with bacterial wall LPS, known to trigger massive ROS production, was used as a positive control.

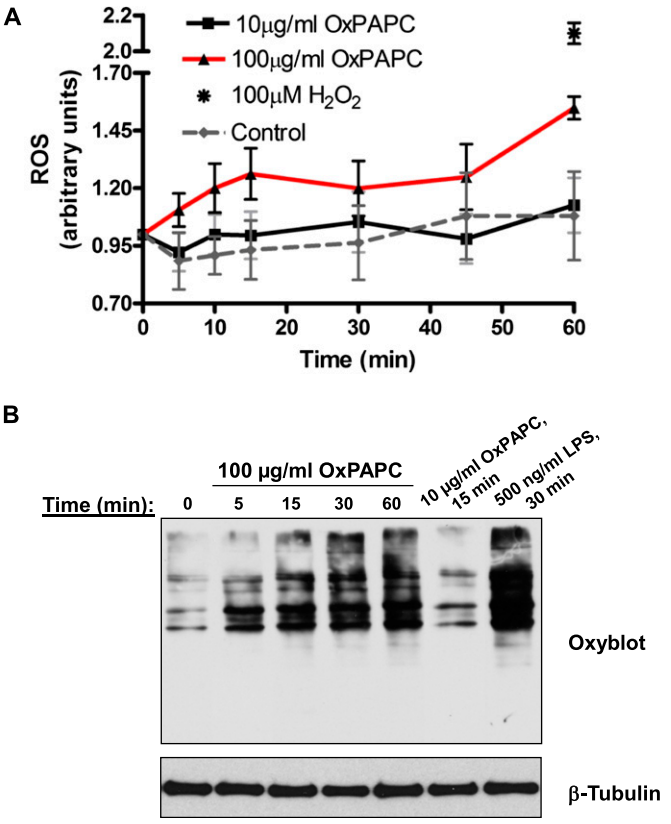

Figure 2. OxPAPC-induced production of reactive oxygen species (ROS) and protein oxidation in OxPAPC-treated ECs. (*A*) Cells were treated with 10 μg/ml or 100 μg/ml OxPAPC, and ROS production was measured with a fluorogenic marker for ROS in live cells (carboxy-2′,7′-dichlorodihydrofluorescein diacetate), as described in MATERIALS AND METHODS. The stimulation of ECs with H_2O_2 (100 μM, 60 minutes), as indicated by an *asterisk*, was used as a positive control. All experiments were repeated three times. Values represent means ± SDs, pooled from three independent experiments. (*B*) Analysis of protein oxidation. Cells were stimulated with 10 μg/ml OxPAPC or 100 μg/ml OxPAPC for different periods of time and lysed. The treatment of ECs with LPS was used as a positive control. Extracted proteins were derivatized with 2,4-dinitrophenylhydrazine (DNPH), electrophoretically separated, blotted, and used for anti-DNPH immunostaining, as described in MATERIALS AND METHODS. The results shown are representative of three independent experiments.

Concentration-Dependent Effects of OxPAPC on AJ Remodeling, Site-Specific VE-Cadherin Phosphorylation, Internalization, and AJ Protein Association

The cellular localization of three principal AJ proteins, VE-cadherin, β-catenin, and p120-catenin in pulmonary ECs treated with high and low OxPAPC doses, was assessed by immunofluorescence staining. Treatment with 10 μg/ml OxPAPC significantly increased β-catenin and VE-cadherin staining at the cell periphery. Merged images revealed β-catenin and VE-cadherin colocalization (Figure 3A). Similarly, 10 μg/ml OxPAPC increased the peripheral accumulation of p120-catenin and its colocalization with VE-cadherin (Figure 3B). In contrast, EC treatment with 100 μg/ml OxPAPC caused the disappearance of peripheral VE-cadherin, β-catenin, and p120-catenin colocalization, which indicates a dissociation of the AJ complexes induced by high OxPAPC concentrations (Figures 3A and 3B, *right*).

To evaluate the potential mechanisms involved in the differential responses of ECs to different concentrations of OxPAPC, we analyzed protein tyrosine phosphorylation in samples from cells stimulated with 10 μg/ml and 100 μg/ml OxPAPC (Figure 4A). OxPAPC at 100 μg/ml caused a time-dependent increase in total protein tyrosine phosphorylation, with the maximum signal achieved at 30 minutes of incubation, whereas a low OxPAPC concentration (10 μg/ml) only modestly increased phosphotyrosine immunoreactivity in stimulated ECs.

VE-cadherin is a key protein in the regulation of endothelial cell–cell interactions and EC barrier function. Tyrosine (Tyr) phosphorylation of VE-cadherin at Tyr^{658} and Tyr^{731} inhibits the formation of AJs (20). We next examined the tyrosine phosphorylation of VE-cadherin at Tyr^{658} and Tyr^{731} in cells treated with barrier-enhancing and barrier-disruptive OxPAPC concentrations. In contrast to low doses of OxPAPC, the treatment of ECs with 100 μg/ml OxPAPC caused rapid and sustained VE-cadherin phosphorylation at both sites (Figure 4B). The immunofluorescence staining of EC monolayers treated with 100 μg/ml OxPAPC revealed increased diffuse cytoplasmic

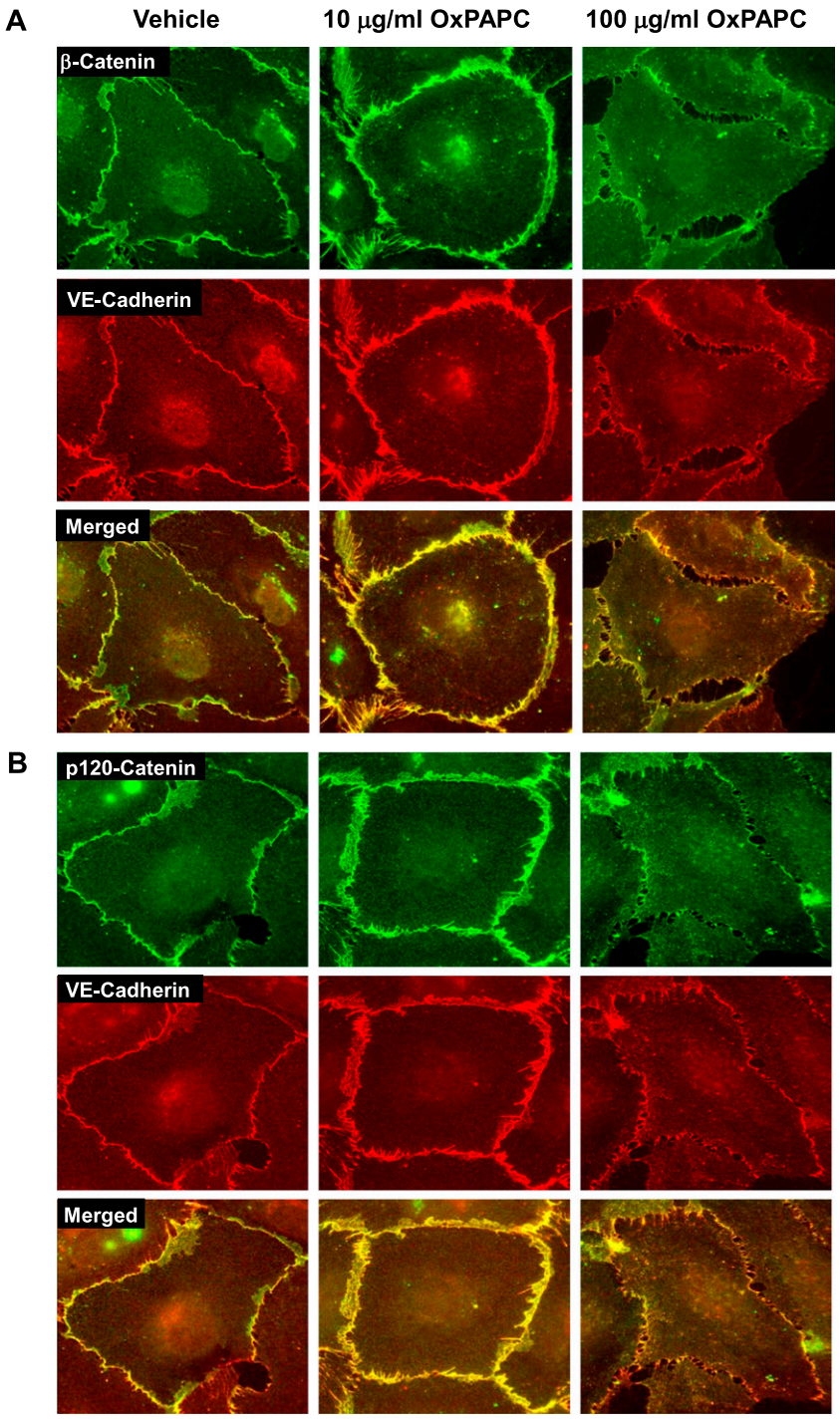

Figure 3. Immunolocalization of p120-catenin and β-catenin in OxPAPC-stimulated ECs. ECs grown on glass coverslips were stimulated with OxPAPC (10 μg/ml or 100 μg/ml, for 30 minutes), followed by double immunofluorescence staining for (*A*) β-catenin (*green*) and VE-cadherin (*red*), and (*B*) p120-catenin (*green*) and VE-cadherin (*red*). Merged images depict areas of protein colocalization, which appear in *yellow*. The results shown are representative of three independent experiments.

phospho-Tyr^{731} VE-cadherin immunoreactivity, without signs of peripheral accumulation (Figure 4C).

The VE-cadherin internalization induced by high OxPAPC concentrations was further verified via the internalization assay described in MATERIALS AND METHODS. After the *in situ* biotinylation of cell-surface proteins in control and OxPAPC-challenged ECs, concentrations of biotinylated VE-cadherin were assessed by Western blotting. The results demonstrated the disappearance of VE-cadherin from the cell surface within minutes after treatment with high OxPAPC doses (Figure 5A). We also examined the effects of high and low OxPAPC doses on the assembly of AJ protein complexes, using coimmunoprecipitation assays. The treatment of ECs with 10 μg/ml OxPAPC significantly increased the association between VE-cadherin, p120-catenin, and β-catenin (Figure 5B). In contrast, the treatment of ECs with 100 μg/ml OxPAPC decreased the association between VE-cadherin, p120-catenin, and β-catenin below the basal levels observed in nonstimulated cells.

Dose-Dependent Effects of OxPAPC on Src Tyrosine Phosphorylation, and the Role of Src and ROS in VE-Cadherin Phosphorylation and Dissociation of AJ Protein

The autophosphorylation of Tyr^{418} within the kinase activation loop is a marker of Src activation. On the other hand, the phosphorylation of Tyr^{529} (the target residue of c-Src tyrosine kinase) promotes intramolecular interactions of the Src COOH terminus with the Src homology-2 domain, effectively inhibiting

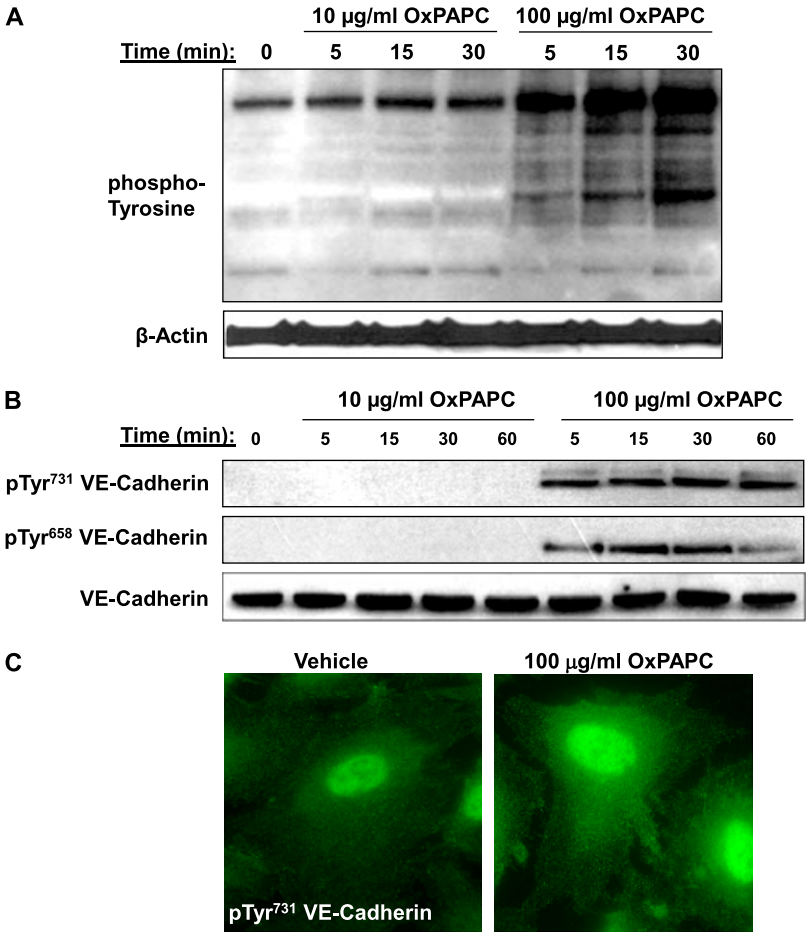

Figure 4. Effects of OxPAPC on total and VE-cadherin–specific tyrosine (Tyr) phosphorylation. (*A*) ECs stimulated with 10 μg/ml or 100 μg/ml OxPAPC for indicated periods of time were lysed and used for immunoblotting analysis with anti-phosphotyrosine antibodies. Staining with β-actin antibody was used as a normalization control. (*B*) ECs were stimulated with OxPAPC (10 μg/ml or 100 μg/ml) for indicated periods of time, and VE-cadherin phosphorylation at Tyr^{731} and Tyr^{731} was examined by Western blot analysis. Staining with VE-cadherin antibody was used as a normalization control. (*C*) ECs were stimulated with 100 μg/ml OxPAPC for 15 minutes, fixed, permeabilized, and stained with anti-$pTyr^{731}$ VE-cadherin antibody. The results shown are representative of three independent experiments. p, phospho.

kinase activity (29, 30). Thus, phosphorylation at Tyr^{529} is a marker of Src suppression. Cells treated with 100 μg/ml OxPAPC revealed a rapid and pronounced phosphorylation of Src at Tyr^{418}, whereas 10 μg/ml OxPAPC caused a much lower increase in phospho-Tyr^{418} immunoreactivity (Figure 6A). Considerable levels of Src phosphorylation at Tyr^{529} were detected in nonstimulated control samples, but were not significantly affected by either high or low concentrations of OxPAPC.

The results of this study indicate that high OxPAPC doses stimulate Src activity and ROS production. We next examined the relationships between Src and ROS signaling, using the Src kinase inhibitor PP2 and the antioxidant agent *N*-acetyl cysteine (NAC). Cell pretreatment with the Src inhibitor PP2 completely abolished OxPAPC-induced Src activation, as measured by autophosphorylation at Tyr^{418}, but the ROS scavenger NAC only partly attenuated this effect of OxPAPC on Src (Figure 6B). These data strongly suggest the existence of additional ROS-independent mechanisms of Src activation by OxPAPC. In turn, the inhibition of Src did not affect the ROS production stimulated by high OxPAPC doses, whereas NAC completely abolished this effect (Figure 6C). These results suggest that Src is not involved in the activation of ROS production by high OxPAPC doses, but can be partly regulated by ROS.

We further studied the involvement of Src-dependent and ROS-dependent pathways in the site-specific tyrosine phosphorylation of VE-cadherin and the interactions of VE-cadherin with p120-catenin and β-catenin. VE-cadherin phosphorylation at Tyr^{731} was significantly reduced by the preincubation of OxPAPC-treated cells with 1 μM PP2 and 1 mM NAC (Figure 6D). Importantly, the dissociation of the VE-cadherin–p120-catenin–β-catenin complex caused by 100 μg/ml OxPAPC was attenuated by the pretreatment of ECs with 1 μM PP2 or 1 mM NAC (Figure 6E). The preincubation of OxPAPC-treated cells with 1 μM PP2 and 1 mM NAC also decreased the drop in transendothelial resistance caused by 100 μg/ml of OxPAPC (Figure 7A). In agreement with the results of permeability studies, preincubation with 1 μM PP2 or 1 mM NAC markedly attenuated the formation of intercellular gaps (Figure 7B) caused by 100 μg/ml OxPAPC, and suppressed the disappearance of VE-cadherin from cell–cell junction areas, reflecting the preservation of AJs (Figure 7C).

DISCUSSION

The effects of oxidized phospholipids, as described *in vitro* and *in vivo*, suggest their potential relevance in different pathologies, including those of atherosclerosis, ischemia/reperfusion injury, acute inflammation, lung injury, and many other conditions (1). Many of the effects of OxPAPC result from changes in endothelial barrier function. In this study, we present data showing that oxidized phospholipids may exert favorable or detrimental effects on endothelial integrity, depending on their concentration, and distinct cellular molecular changes are involved in this differential regulation, as effected by high and low concentrations of OxPAPC.

The question regarding OxPL concentrations in the circulation and in target organs under physiologic and in specific pathologies remains open. Published measurements differ significantly, and often represent different OxPL species measured in different body compartments. However, in previous reports, substantial amounts of oxidized phospholipids such as $oxPC_{CD36}$ (a novel family of oxidized choline glycerophospholipids that are

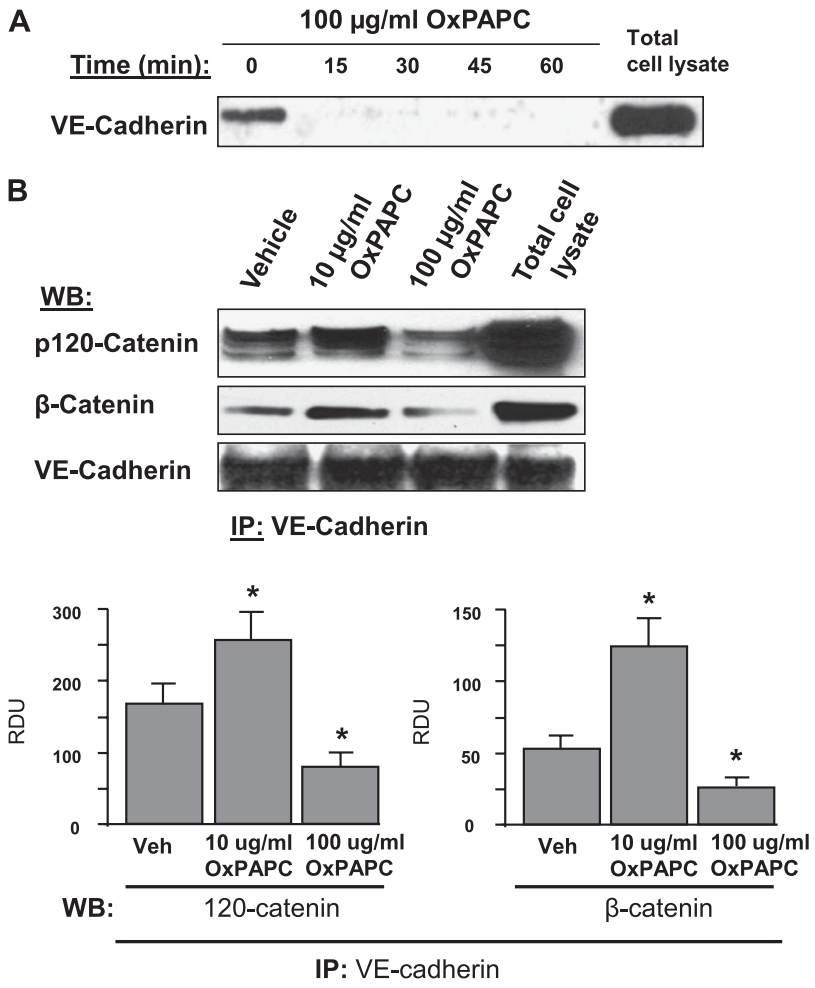

Figure 5. Effects of OxPAPC on VE-cadherin internalization and interaction with β-catenin and p120-catenin. (*A*) Cells were stimulated with OxPAPC for indicated periods of time and washed, and cell-surface proteins were labeled with Sulfo-NHS-SS-Biotin, as described in MATERIALS AND METHODS. Cells were lysed, and biotinylated proteins were precipitated with streptavidin–agarose. The presence of biotinylated VE-cadherin was evaluated by Western blot analysis. (*B*) VE-cadherin was immunoprecipitated from cells stimulated with OxPAPC (10 μg/ml or 100 μg/ml, 30 minutes). Amounts of coimmunoprecipitated p120-catenin and β-catenin were evaluated by Western blot analysis. The bar graph depicts results of quantitative analyses of VE-cadherin–p120-catenin and VE-cadherin–β-catenin associations. All experiments were repeated three times. Values are mean ± SD. *$P < 0.05$, versus control samples. IP, immunoprecipitation; Veh, vehicle; WB, western blot.

enriched within atheromas and serve as specific high-affinity ligands for macrophage CD36) and its oxidation products (such as 1-palmitoyl-2-(5-oxovaleroyl)-*sn*-glycero-3-phosphocholine and 1-palmitoyl-2-glutaroyl-*sn*-glycero-3-phosphocholine [PGPC]) were detected in all human samples tested, and the combined concentration of all oxidized phospholipids ranged from 5.4–51 μM (31, 32). The concentrations of OxPAPC used in this study ranged from 10–50 μg/ml. Using an average molecular mass of 609 g/mol for major OxPAPC compounds such as PGPC results in an estimated range of OxPAPC molar concentrations within 16–80 μM. Concentrations of OxPL in normal human plasma were estimated at a range of 0.1–1.0 μM (33), but local tissue concentrations in atherosclerotic regions of vessels were reported at a range of 10–100 μM/kg (13, 25). However, OxPAPC is a very complex mixture of oxidized phospholipid products, with molecular masses in the range of 300 to more than 1,000. Therefore, the OxPAPC concentrations used in our experiments fell within the range of OxPAPC reported in the literature in different tissues, and we speculate that our results may have future implications in the development of new therapies based on taking advantage of the beneficial properties of oxidized phospholipids, and in approaches to eliminating the detrimental effects inherent in some fractions of OxPAPC.

The peripheral actin cytoskeleton and cell–cell junctions play a critical role in the maintenance of endothelial monolayer integrity (20, 34). OxPAPC at low concentrations promotes EC barrier enhancement by strengthening the peripheral actin rim and stimulating the Rap–Rac-dependent assembly of AJs and tight junction complexes (21, 35). In contrast, higher OxPAPC concentrations led to EC barrier dysfunction, and the mechanisms underlying this dysfunction remain unclear. The present study shows that the rapid barrier dysfunction induced by high doses of OxPAPC was associated with decreased VE-cadherin–β-catenin–p120-catenin interactions and the disappearance of VE-cadherin from cell–cell junction areas. The destabilization of AJs is an important mechanism of increased EC permeability (34), and was also described for other edemagenic and inflammatory agents such as TNF-α (36), platelet-activating factor (37), and vascular endothelial growth factor (VEGF) (38).

Our proteomics experiments in human aortic ECs treated with 50 μg/ml OxPAPC (for 40 minutes) demonstrated a large increase in both the tyrosine and serine phosphorylation of a number of proteins, including VE-cadherin (39). Our present data indicate that the extent of total protein tyrosine phosphorylation and VE-cadherin tyrosine phosphorylation differs significantly between cells treated with 10 μg/ml and 100 μg/ml of OxPAPC. This study also shows that OxPAPC at barrier-disruptive concentrations promotes the phosphorylation of VE-cadherin at Tyr^{658} and Tyr^{731}, whereas at low doses, OxPAPC does not induce this effect. VE-cadherin phosphorylation at these two critical tyrosines is sufficient to prevent the binding of p120-catenin and β-catenin, respectively, to the cytoplasmic tail of VE-cadherin. Furthermore, phosphorylation at either site leads to the inhibition of cell barrier function (40, 41). Our coimmunoprecipitation and microscopy data indicate that low OxPAPC concentrations increased the association of p120-catenin and VE-cadherin, whereas treatment with high OxPAPC concentrations led to the disassembly of these

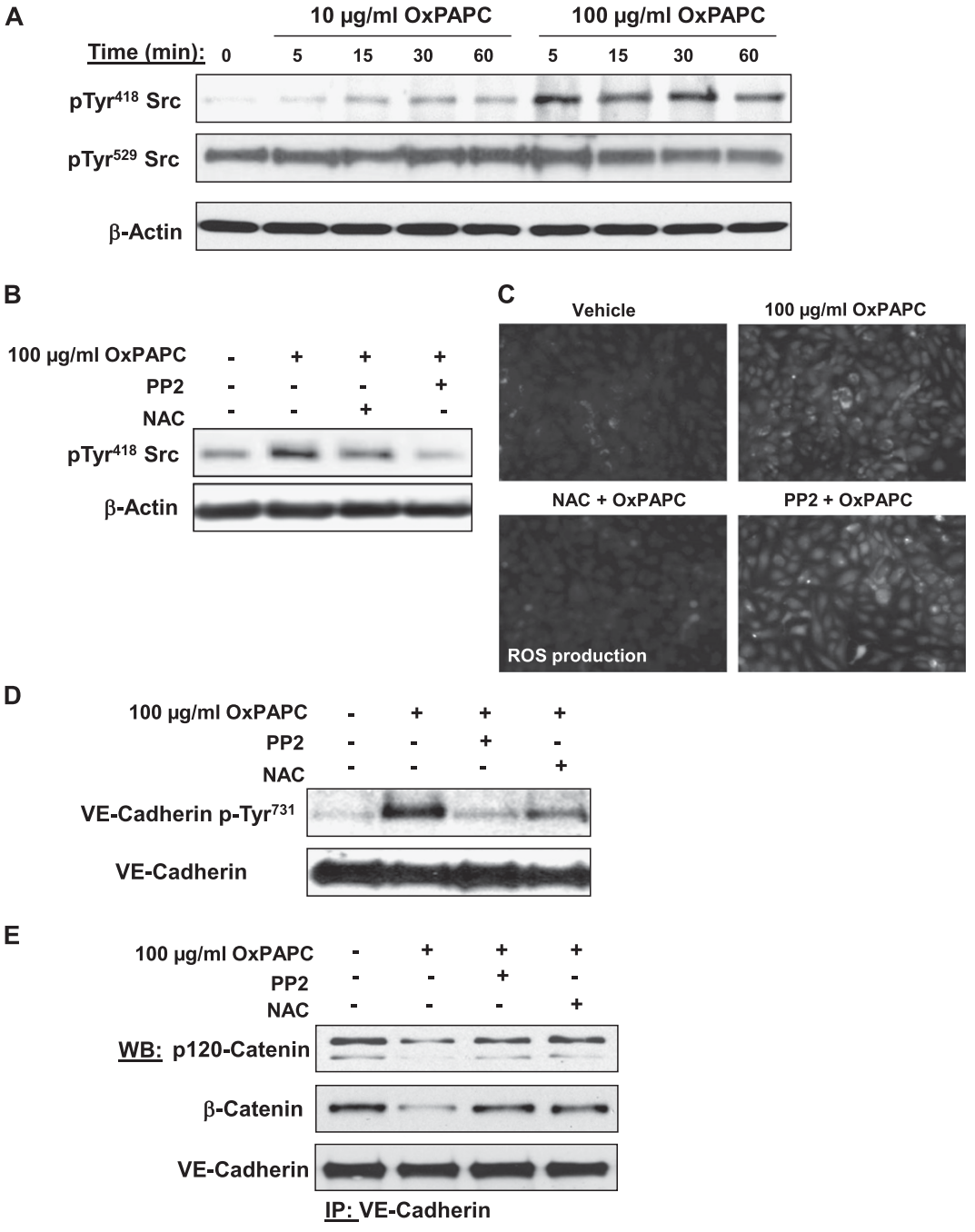

Figure 6. Analysis of OxPAPC-induced Src phosphorylation and effects of Src and ROS inhibitors on VE-cadherin phosphorylation and the formation of VE-cadherin–p120-catenin–β-catenin complexes. (*A*) HPAECs were stimulated with OxPAPC (10 μg/ml or 100 μg/ml) for indicated periods of time, and Src phosphorylation at Tyr^{418} and Tyr^{529} was examined by Western blot analysis. Staining with β-actin antibody was used as a normalization control. (*B–D*) Cells pretreated with vehicle, Src inhibitor PP2 (1μM), or the antioxidant *N*-acetyl-cysteine (NAC; 1 mM) for 30 minutes were stimulated with OxPAPC (100 μg/ml, 15 minutes). Concentrations of Src phosphorylation at Tyr^{418} were detected by Western blot analysis. (*B*) Staining with β-actin antibody was used as a normalization control. (*C*) The assay of ROS production was performed as described in MATERIALS AND METHODS. (*D*) Concentrations of VE-cadherin phosphorylated at Tyr^{731} were detected by Western blot analysis. (*E*) Cells pretreated with vehicle, PP2 (1 μM), or NAC (1 mM) for 30 minutes were stimulated with OxPAPC (100 μg/ml, 15 minutes), followed by immunoprecipitation with anti–VE-cadherin antibody. Coimmunoprecipiated p120-catenin and β-catenin were detected by Western blot analysis with corresponding antibodies. The detection of immunoprecipiated VE-cadherin was used as a normalization control. The results shown are representative of five independent experiments.

complexes. These results support the hypothesis that high OxPAPC concentrations cause the tyrosine phosphorylation of VE-cadherin and the disassembly of p120-catenin–β-catenin–VE-cadherin complexes, with a subsequent destabilization of intercellular VE-cadherin bridges and the disappearance of VE-cadherin from the cell surface.

The exact mechanism of VE-cadherin phosphorylation induced by high OxPAPC concentrations remains to be elucidated. Our previous study demonstrated that a rapid activation of Src was required for the induction of IL-8 synthesis by OxPAPC (40 μg/ml) (11). The present study revealed early Src phosphorylation at Tyr^{418}, leading to Src activation in ECs treated with high OxPAPC concentrations, but no changes in phosphorylation at Tyr^{529}, reflecting the down-regulation of Src enzymatic activity (29, 30). Thus, the rapid activation of Src caused by high OxPAPC concentrations is consistent with the time course of VE-cadherin phosphorylation, and with the attenuation of VE-cadherin phosphorylation by the Src inhibitor PP2. These changes also correlate with OxPAPC-induced EC permeability, suggesting a role for Src kinase activation in the disassembly of AJs and the endothelial barrier dysfunction induced by high OxPAPC concentrations. Previous reports demonstrated the activation of Src and Rac GTPase by both low and high OxPAPC concentrations, which led to opposing effects on EC permeability. How can these findings be reconciled? The moderate stimulation of Src activity during OxPAPC treatment at barrier-protective concentrations (23, 42) does not induce VE-cadherin phosphorylation (according to the present study), but does induce the tyrosine phosphorylation of the Src downstream targets paxillin (42) and p190RhoGAP (24), required for a maximal EC barrier–enhancing response to OxPAPC (24). In turn, the strong tyrosine phosphorylation of the other Src target

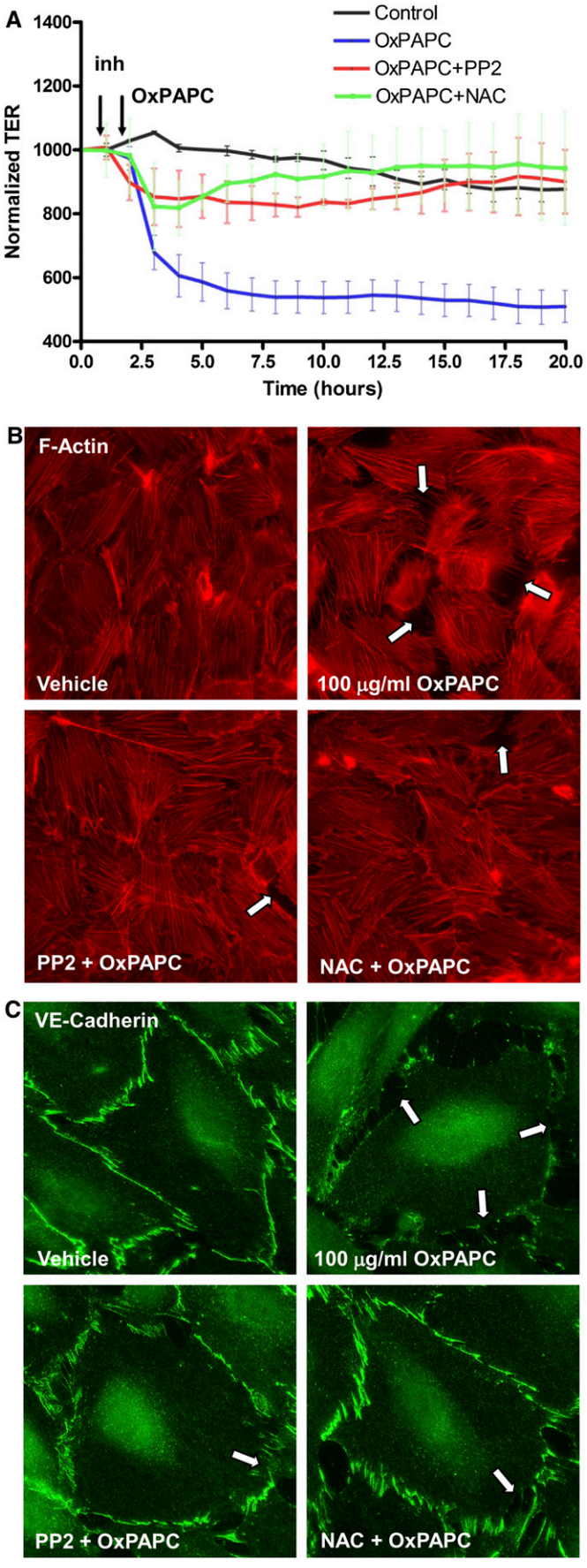

Figure 7. Effects of Src and ROS inhibitors on EC permeability and monolayer disruption induced by 100 μg/ml OxPAPC. HPAECs were pretreated with vehicle, PP2 (1 μM), or NAC (1 mM) for 30 minutes, followed by stimulation with 100 μg/ml OxPAPC. (*A*) Measurements of TER were monitored for 20 hours. The data shown here were pooled from three independent experiments, and are expressed as means ± SD. (*B* and *C*) Immunofluorescence staining for F-actin (*B*) or VE-cadherin (*C*) was performed after 15 minutes of OxPAPC stimulation. *Arrows* indicate areas of intercellular gaps. The results shown are representative of three independent experiments.

VE-cadherin by high OxPAPC doses was demonstrated this study, and was linked to a barrier-disruptive response.

Increased ROS production appears to be responsible for some mechanisms of OxPAPC action. OxPAPC was shown to induce vascular endothelial peroxide production by activating the nicotinamide adenine dinucleotide phosphate–reduced (NADPH) oxidase complex. The knockdown of NADPH oxidase isoform-4 and its components Rac-1 and p22(phox) decreased the induction by OxPAPC of inflammatory and sterol regulatory genes, but did not affect OxPAPC's transcriptional regulation of antioxidant genes and the unfolded protein response (14, 15). The Rac-1/NADPH–dependent generation of ROS may also promote EC permeability. The enzymatic generation of superoxide by xanthine oxidase was also increased nearly twofold after the exposure of bovine aortic ECs to OxPAPC and increased occludin phosphorylation, thus implicating ROS in the OxPAPC-mediated control of tight junctions (43). The results of the present study indicate that high OxPAPC concentrations trigger the production of ROS and protein oxidation, whereas barrier-enhancing low OxPAPC concentrations do not significantly elevate ROS.

The pretreatment of EC with NAC reversed the increases in EC permeability and the disassembly of p120-catenin–VE-cadherin complexes caused by high OxPAPC concentrations, and suppressed VE-cadherin phosphorylation at Tyr^{658} and Tyr^{731}. These results are in agreement with other reports on the protective effects of the ROS inhibitors superoxide dismutase and catalase against the phosphorylation and degradation of tight junction protein occludin contributing to the endothelial barrier disruption caused by elevated OxPAPC concentrations (43). Interestingly, pretreatment with NAC only partly decreased OxPAPC-induced Src autophosphorylation at Tyr^{418}. Previous data demonstrated that the redox-dependent inactivation of low molecular weight protein tyrosine phosphatase (LMW-PTP) was implicated in regulating levels of tyrosine phosphorylation and the activity of signaling kinases, including Src (44–46), and in controlling cell junction complex integrity (47, 48). Thus, we speculate that the ROS-dependent inactivation of LMW-PTP in ECs exposed to high OxPAPC doses may contribute to sustained VE-cadherin phosphorylation via their promotional effects on Src activity, but this ROS-dependent inactivation of LMW-PTP may also stimulate additional mechanisms leading to increased VE-cadherin phosphorylation. Other experiments showed that PP2 did not affect the production of ROS caused by high OxPAPC concentrations. Together, these data suggest an Src-independent mechanism of ROS production and a partial regulation of Src activity by activated redox signaling induced by high OxPAPC doses.

On the other hand, Rac-1 is a subunit of the NADPH oxidase complex required for the activation of NADPH oxidase and production of ROS. Rac-1/NADPH–mediated ROS generation induced the tyrosine phosphorylation of VE-cadherin and β-catenin, and was also implicated in the endothelial permeability

caused by VEGF (49). On the other hand, an increased production of ROS stimulates redox-sensitive tyrosine kinase activities and inhibits low molecular weight protein tyrosine phosphatases, through a mechanism referred to as the Bar-Sagi pathway (50). VE-cadherin–specific protein tyrosine phosphatase may be one of the targets of ROS, leading to VE-cadherin hyperphosphorylation. These events trigger a vicious circle of ROS–tyrosine kinase signaling, leading to EC barrier dysfunction, inflammatory gene expression, and other pathologic effects. The increased tyrosine phosphorylation of VE-cadherin in murine tissues in cancer and in angiogenic and ischemic conditions associated with increased vascular leakiness (51–53) emphasizes the importance of this mechanism in the propagation of disease states. The excessive production of ROS may also trigger additional signaling mechanisms that override the barrier-protective pathways induced by Rac. Thus, a delicate balance of Rac and tyrosine kinase activities and subcellular compartmentalization may define the permeability responses of ECs exposed to different OxPAPC concentrations.

In conclusion, this study demonstrates that in contrast to OxPAPC at low concentrations, OxPAPC at high doses causes a rapid increase in endothelial permeability. This mechanism does not implicate an activation of actomyosin contraction, but involves the rapid activation of ROS production and the phosphorylation of Src kinase, leading to the phosphorylation of VE-cadherin at Tyr^{658} and Tyr^{731}, the disassembly of VE-cadherin–p120-catenin–β-catenin cell–cell junction complexes, and EC monolayer barrier compromise. The mechanisms mediating the sustained increase in EC permeability caused by high OxPAPC doses may engage additional signaling systems. These mechanisms remain to be investigated. Advances in the knowledge of signaling pathways and mechanisms triggered by circulating oxidized phospholipids and their role in the control of endothelial permeability and inflammatory processes in various diseases may play an important part in the development of new therapeutic options.

Author disclosures are available with the text of this article at www.atsjournals.org.

Acknowledgments: The authors thank Nurgul Moldobaeva for superb laboratory assistance.

References

1. Bochkov VN, Oskolkova OV, Birukov KG, Levonen AL, Binder CJ, Stockl J. Generation and biological activities of oxidized phospholipids. *Antioxid Redox Signal* 2010;12:1009–1059.
2. Chabot F, Mitchell JA, Gutteridge JM, Evans TW. Reactive oxygen species in acute lung injury. *Eur Respir J* 1998;11:745–757.
3. Lang JD, McArdle PJ, O'Reilly PJ, Matalon S. Oxidant–antioxidant balance in acute lung injury. *Chest* 2002;122:314S–320S.
4. Wood LG, Gibson PG, Garg ML. Biomarkers of lipid peroxidation, airway inflammation and asthma. *Eur Respir J* 2003;21:177–186.
5. Berliner JA, Gharavi NM. Endothelial cell regulation by phospholipid oxidation products. *Free Radic Biol Med* 2008;45:119–123.
6. Imai Y, Kuba K, Neely GG, Yaghubian-Malhami R, Perkmann T, van Loo G, Ermolaeva M, Veldhuizen R, Leung YH, Wang H, *et al*. Identification of oxidative stress and Toll-like receptor 4 signaling as a key pathway of acute lung injury. *Cell* 2008;133:235–249.
7. Ma Z, Li J, Yang L, Mu Y, Xie W, Pitt B, Li S. Inhibition of LPS- and CPG DNA–induced TNF-alpha response by oxidized phospholipids. *Am J Physiol Lung Cell Mol Physiol* 2004;286:L808–L816.
8. Nonas S, Birukova AA, Fu P, Xing J, Chatchavalvanich S, Bochkov VN, Leitinger N, Garcia JG, Birukov KG. Oxidized phospholipids reduce ventilator-induced vascular leak and inflammation *in vivo*. *Crit Care* 2008;12:R27.
9. Nonas SA, Miller I, Kawkitinarong K, Chatchavalvanich S, Gorshkova I, Bochkov VN, Leitinger N, Natarajan V, Garcia JG, Birukov KG. Oxidized phospholipids reduce vascular leak and inflammation in rat model of acute lung injury. *Am J Respir Crit Care Med* 2006;173:1130–1138.
10. Lee H, Shi W, Tontonoz P, Wang S, Subbanagounder G, Hedrick CC, Hama S, Borromeo C, Evans RM, Berliner JA, *et al*. Role for peroxisome proliferator–activated receptor alpha in oxidized phospholipid-induced synthesis of monocyte chemotactic protein–1 and interleukin-8 by endothelial cells. *Circ Res* 2000;87:516–521.
11. Yeh M, Gharavi NM, Choi J, Hsieh X, Reed E, Mouillesseaux KP, Cole AL, Reddy ST, Berliner JA. Oxidized phospholipids increase interleukin 8 (IL-8) synthesis by activation of the c-SRC/signal transducers and activators of transcription (STAT)3 pathway. *J Biol Chem* 2004;279:30175–30181.
12. Shih PT, Elices MJ, Fang ZT, Ugarova TP, Strahl D, Territo MC, Frank JS, Kovach NL, Cabanas C, Berliner JA, *et al*. Minimally modified low-density lipoprotein induces monocyte adhesion to endothelial connecting segment–1 by activating beta1 integrin. *J Clin Invest* 1999;103:613–625.
13. Subbanagounder G, Leitinger N, Schwenke DC, Wong JW, Lee H, Rizza C, Watson AD, Faull KF, Fogelman AM, Berliner JA. Determinants of bioactivity of oxidized phospholipids: specific oxidized fatty acyl groups at the SN-2 position. *Arterioscler Thromb Vasc Biol* 2000;20:2248–2254.
14. Lee S, Gharavi NM, Honda H, Chang I, Kim B, Jen N, Li R, Zimman A, Berliner JA. A role for NADPH oxidase 4 in the activation of vascular endothelial cells by oxidized phospholipids. *Free Radic Biol Med* 2009;47:145–151.
15. Rouhanizadeh M, Hwang J, Clempus RE, Marcu L, Lassegue B, Sevanian A, Hsiai TK. Oxidized-1-palmitoyl-2-arachidonoyl-*sn*-glycero-3-phosphorylcholine induces vascular endothelial superoxide production: implication of NADPH oxidase. *Free Radic Biol Med* 2005;39:1512–1522.
16. Ohkura N, Hiraishi S, Itabe H, Hamuro T, Kamikubo Y, Takano T, Matsuda J, Horie S. Oxidized phospholipids in oxidized low-density lipoprotein reduce the activity of tissue factor pathway inhibitor through association with its carboxy-terminal region. *Antioxid Redox Signal* 2004;6:705–712.
17. Marathe GK, Zimmerman GA, Prescott SM, McIntyre TM. Activation of vascular cells by PAF-like lipids in oxidized LDL. *Vascul Pharmacol* 2002;38:193–200.
18. Bochkov VN, Kadl A, Huber J, Gruber F, Binder BR, Leitinger N. Protective role of phospholipid oxidation products in endotoxin-induced tissue damage. *Nature* 2002;419:77–81.
19. Birukov KG, Bochkov VN, Birukova AA, Kawkitinarong K, Rios A, Leitner A, Verin AD, Bokoch GM, Leitinger N, Garcia JG. Epoxycyclopentenone-containing oxidized phospholipids restore endothelial barrier function via Cdc42 and Rac. *Circ Res* 2004;95:892–901.
20. Dejana E, Orsenigo F, Lampugnani MG. The role of adherens junctions and VE-cadherin in the control of vascular permeability. *J Cell Sci* 2008;121:2115–2122.
21. Birukova AA, Malyukova I, Poroyko V, Birukov KG. Paxillin–{beta}-catenin interactions are involved in Rac/Cdc42–mediated endothelial barrier–protective response to oxidized phospholipids. *Am J Physiol Lung Cell Mol Physiol* 2007;293:L199–L211.
22. Birukova AA, Fu P, Chatchavalvanich S, Burdette D, Oskolkova O, Bochkov VN, Birukov KG. Polar head groups are important for barrier protective effects of oxidized phospholipids on pulmonary endothelium. *Am J Physiol Lung Cell Mol Physiol* 2007;292:L924–L935.
23. Birukova AA, Chatchavalvanich S, Oskolkova O, Bochkov VN, Birukov KG. Signaling pathways involved in OxPAPC-induced pulmonary endothelial barrier protection. *Microvasc Res* 2007;73:173–181.
24. Birukova AA, Zebda N, Cokic I, Fu P, Wu T, Dubrovskyi O, Birukov KG. p190RhoGAP mediates protective effects of oxidized phospholipids in the models of ventilator-induced lung injury. *Exp Cell Res* 2011;317:859–872.
25. Watson AD, Leitinger N, Navab M, Faull KF, Horkko S, Witztum JL, Palinski W, Schwenke D, Salomon RG, Sha W, *et al*. Structural identification by mass spectrometry of oxidized phospholipids in minimally oxidized low density lipoprotein that induce monocyte/endothelial interactions and evidence for their presence *in vivo*. *J Biol Chem* 1997;272:13597–13607.
26. Birukov KG, Jacobson JR, Flores AA, Ye SQ, Birukova AA, Verin AD, Garcia JG. Magnitude-dependent regulation of pulmonary endothelial

cell barrier function by cyclic stretch. *Am J Physiol Lung Cell Mol Physiol* 2003;285:L785–L797.
27. Birukova AA, Smurova K, Birukov KG, Kaibuchi K, Garcia JGN, Verin AD. Role of Rho GTPases in thrombin-induced lung vascular endothelial cells barrier dysfunction. *Microvasc Res* 2004;67:64–77.
28. Leitinger N, Tyner TR, Oslund L, Rizza C, Subbanagounder G, Lee H, Shih PT, Mackman N, Tigyi G, Territo MC, *et al*. Structurally similar oxidized phospholipids differentially regulate endothelial binding of monocytes and neutrophils. *Proc Natl Acad Sci USA* 1999;96:12010–12015.
29. Xu W, Doshi A, Lei M, Eck MJ, Harrison SC. Crystal structures of c-SRC reveal features of its autoinhibitory mechanism. *Mol Cell* 1999; 3:629–638.
30. Young MA, Gonfloni S, Superti-Furga G, Roux B, Kuriyan J. Dynamic coupling between the SH2 and SH3 domains of c-SRC and HCK underlies their inactivation by c-terminal tyrosine phosphorylation. *Cell* 2001;105:115–126.
31. Podrez EA, Byzova TV, Febbraio M, Salomon RG, Ma Y, Valiyaveettil M, Poliakov E, Sun M, Finton PJ, Curtis BR, *et al*. Platelet CD36 links hyperlipidemia, oxidant stress and a prothrombotic phenotype. *Nat Med* 2007;13:1086–1095.
32. Hammad LA, Wu G, Saleh MM, Klouckova I, Dobrolecki LE, Hickey RJ, Schnaper L, Novotny MV, Mechref Y. Elevated levels of hydroxylated phosphocholine lipids in the blood serum of breast cancer patients. *Rapid Commun Mass Spectrom* 2009;23:863–876.
33. Oskolkova OV, Afonyushkin T, Preinerstorfer B, Bicker W, von Schlieffen E, Hainzl E, Demyanets S, Schabbauer G, Lindner W, Tselepis AD, *et al*. Oxidized phospholipids are more potent antagonists of lipopolysaccharide than inducers of inflammation. *J Immunol* 2010;185:7706–7712.
34. Mehta D, Malik AB. Signaling mechanisms regulating endothelial permeability. *Physiol Rev* 2006;86:279–367.
35. Birukova AA, Zebda N, Fu P, Poroyko V, Cokic I, Birukov KG. Association between adherens junctions and tight junctions via Rap1 promotes barrier protective effects of oxidized phospholipids. *J Cell Physiol* 2011;226:2052–2062.
36. Angelini DJ, Hyun SW, Grigoryev DN, Garg P, Gong P, Singh IS, Passaniti A, Hasday JD, Goldblum SE. TNF-alpha increases tyrosine phosphorylation of vascular endothelial cadherin and opens the paracellular pathway through Fyn activation in human lung endothelia. *Am J Physiol Lung Cell Mol Physiol* 2006;291:L1232–L1245.
37. Hudry-Clergeon H, Stengel D, Ninio E, Vilgrain I. Platelet-activating factor increases VE-cadherin tyrosine phosphorylation in mouse endothelial cells and its association with the PTDINS3′-kinase. *FASEB J* 2005;19:512–520.
38. Esser S, Lampugnani MG, Corada M, Dejana E, Risau W. Vascular endothelial growth factor induces VE-cadherin tyrosine phosphorylation in endothelial cells. *J Cell Sci* 1998;111:1853–1865.
39. Zimman A, Chen SS, Komisopoulou E, Titz B, Martinez-Pinna R, Kafi A, Berliner JA, Graeber TG. Activation of aortic endothelial cells by oxidized phospholipids: a phosphoproteomic analysis. *J Proteome Res* 2010;9:2812–2824.
40. Alcaide P, Newton G, Auerbach S, Sehrawat S, Mayadas TN, Golan DE, Yacono P, Vincent P, Kowalczyk A, Luscinskas FW. p120-catenin regulates leukocyte transmigration through an effect on VE-cadherin phosphorylation. *Blood* 2008;112:2770–2779.
41. Potter MD, Barbero S, Cheresh DA. Tyrosine phosphorylation of VE-cadherin prevents binding of p120- and beta-catenin and maintains the cellular mesenchymal state. *J Biol Chem* 2005;280: 31906–31912.
42. Birukov KG, Leitinger N, Bochkov VN, Garcia JG. Signal transduction pathways activated in human pulmonary endothelial cells by OxPAPC, a bioactive component of oxidized lipoproteins. *Microvasc Res* 2004;67:18–28.
43. DeMaio L, Rouhanizadeh M, Reddy S, Sevanian A, Hwang J, Hsiai TK. Oxidized phospholipids mediate occludin expression and phosphorylation in vascular endothelial cells. *Am J Physiol Heart Circ Physiol* 2006;290:H674–H683.
44. Lee JK, Edderkaoui M, Truong P, Ohno I, Jang KT, Berti A, Pandol SJ, Gukovskaya AS. NADPH oxidase promotes pancreatic cancer cell survival via inhibiting Jak2 dephosphorylation by tyrosine phosphatases. *Gastroenterology* 2007;133:1637–1648.
45. Chiarugi P. The redox regulation of LMW-PTP during cell proliferation or growth inhibition. *IUBMB Life* 2001;52:55–59.
46. Chiarugi P, Cirri P, Marra F, Raugei G, Fiaschi T, Camici G, Manao G, Romanelli RG, Ramponi G. The Src and signal transducers and activators of transcription pathways as specific targets for low molecular weight phosphotyrosine–protein phosphatase in platelet-derived growth factor signaling. *J Biol Chem* 1998;273:6776–6785.
47. Taddei ML, Chiarugi P, Cuevas C, Ramponi G, Raugei G. Oxidation and inactivation of low molecular weight protein tyrosine phosphatase by the anticancer drug aplidin. *Int J Cancer* 2006;118:2082–2088.
48. Taddei ML, Chiarugi P, Cirri P, Buricchi F, Fiaschi T, Giannoni E, Talini D, Cozzi G, Formigli L, Raugei G, *et al*. Beta-catenin interacts with low-molecular-weight protein tyrosine phosphatase leading to cadherin-mediated cell–cell adhesion increase. *Cancer Res* 2002;62:6489–6499.
49. Monaghan-Benson E, Burridge K. The regulation of vascular endothelial growth factor–induced microvascular permeability requires Rac and reactive oxygen species. *J Biol Chem* 2009;284:25602–25611.
50. Nimnual AS, Taylor LJ, Bar-Sagi D. Redox-dependent downregulation of Rho by Rac. *Nat Cell Biol* 2003;5:236–241.
51. Lambeng N, Wallez Y, Rampon C, Cand F, Christe G, Gulino-Debrac D, Vilgrain I, Huber P. Vascular endothelial–cadherin tyrosine phosphorylation in angiogenic and quiescent adult tissues. *Circ Res* 2005;96:384–391.
52. Weis S, Cui J, Barnes L, Cheresh D. Endothelial barrier disruption by VEGF-mediated Src activity potentiates tumor cell extravasation and metastasis. *J Cell Biol* 2004;167:223–229.
53. Weis S, Shintani S, Weber A, Kirchmair R, Wood M, Cravens A, McSharry H, Iwakura A, Yoon YS, Himes N, *et al*. Src blockade stabilizes a FLK/cadherin complex, reducing edema and tissue injury following myocardial infarction. *J Clin Invest* 2004;113:885–894.